Patterns in alpha-tubulin fluorescence as a useful predictor of cell cycle stage

Matthew Sexton

Independent Research Project Report

Bio254 – Developmental Biology

May 3, 2012

Introduction

Healthcare and biological research have an ever more important role in the economy and the society. Because of extensive research and increased medical testing tests that doctors and researchers need to perform, there is an increasing shortage of skilled laborers available to spend hours analyzing the multitudes of samples (Kivity et al, 2011). A shortage of laborers who devote their time to the analysis of biological samples is not a problem that the scientific community can solve easily. Other industries have found that turning to technology is a solution that can save time and resources. The decision to automate a process in manufacturing eliminates human workers and replaces them with computer-controlled machines capable of working tirelessly with amazing accuracy and precision. Automating analyses could do the same for biology; providing practical means to address the large quantities of samples without spending more on education and employment (Melegari, Bonaguri, Russo, Luista, Trenti, Lippi, 2012). In addition to saving time and money, automating biological analyses would remove human subjectivity. If every lab is using machines running similar programs that relate experimental data to similar standards, then the results will be relatively free of variation (Melegari, Bonaguri, Russo, Luista, Trenti, Lippi, 2012). An example of successful automation is the automated method for the quantitative analysis of tumor vascularization in renal cancer (Mertz et al, 2007). A potential area for automation in biology is the identification of cell cycle phase. I hypothesize that patterns in α-tubulin arrangement in sea urchin embryos are useful predictors of mitotic phase and provide quantitative results that could lead to an automated process for determining the phase of the cell cycle.

The cell cycle contains multiple stages. There is a growth phase followed by the duplication of duplicate deoxyribonucleic acid (DNA) and then a second growth phase. The two growth phases and synthesis of DNA together make up interphase. Then there is mitosis, which has five distinguishable stages including prophase, prometaphase, metaphase, anaphase, and telophase (Nigg, 2001). Visible features characterize each stage of the cycle and allow researchers to assign any cell to a part to one stage (Nigg, 2001). An integral feature of the cell cycle is the role microtubules (Amos, 2005).

Microtubules are made of α-tubulin and β-tubulin and play roles in mitosis such as making the structural components such as the centrioles and spindle fibers. The centrioles and spindle fibers of a cell are not stationary during mitosis. Instead, the centrioles contained within the centromeres must travel from a central location in the cell to the poles of the cells while the microtubules grow longer and shorter to move the DNA (Nigg, 2001). As a result, it is likely, that each period of the cell cycle will have a characteristic arrangement of microtubules. In this study, we immunofluorescently labeled sea urchin embryos to detect patterns in α-tubulin arrangement and concentration, as measured by brightness of the green fluorescence, in order to determine if there are certain arrangements that characterize different parts of the cell cycle.

Materials and Methods

The procedure for "Immunoflour staining of SU embryos – MeOH fixation" modifications as described (Morris, 2012). In B15, a drop of the polylysine was placed on the bottom of a petri dish and a coverslip placed on top of the drop for one day. Instead of B16, distilled water was dripped at the edge of, and then wicked under, each coverslip. For B17, PBS-T was added to the coverslips, and then refrigerated for three days. To remove a coverslip from a well the solution was removed with a pipette so that liquid just covered the coverslip. The coverslip was then gently lifted out of the well. A 6-well plate was used instead of a humidity chamber until step E26.

In D21, 4.5 µl of Hoechst stock solution was added to 45 ml of block buffer to make a 1 µg/ml solution of Hoechst in block buffer. In D23 the solution was made to be 1:500 and 12 µl of anti-acetylated tubulin antibody (t6793 manufactured by Sigma Chemical Company) was used. The FITC-DM1A anti-alpha tubulin antibody solution in D24 was made 1:50 so that 80 µL of FITC-DM1A was added to 4 ml of block buffer. In D25, 4 µl of Alexaflour 546 Goat anti-mouse secondary antibody (AF546 GAM, catalog number A11003) manufactured by Invitrogen was added to 4 ml of block buffer to make a 1:1000 dilution of AF546 GAM.

E26 and E27 were combined and all coverslips got anti-acetylated tubulin antibody and then incubated for approximately eight hours. After F35, the coverslips were returned to the wells in block bugger and refrigerated for two days. In G38 secondary antibody was not added to the control coverslip. For G40, the incubation was three hours long. The incubation time in step I50 was approximately one hour. In step 60, the chipchamber was sealed with nail polish.

The control group of this procedure is the coverslip that did not receive all of the antibodies or the Hoechst DNA stain while the experimental coverslips were labeled will labeled with all of the antibodies and the Hoechst DNA stain. The control was necessary to confirm that the embryos do not auto-fluoresce and therefore ensure that the observed fluorescence is a result of this procedure.

The experimental slides were viewed on a Nikon Eclipse 80i, first under transmitted light during which the slide was

scanned for interesting embryos. A picture was taken for the transmitted light. Without moving the slide, the embryos were briefly exposed to and photographed under ultraviolet light, blue light, and green light. In between each photograph under the same light, the stage height and exposure was adjusted. Between each type of light, image settings on the computer were changed to reflect the color of light emitted by the sample. The pictures were taken using the Apple iMac Zodiac in the Wheaton College Imaging Center for Undergraduate Collaboration (ICUC) with the software Spot Advanced version 4.6.

To create the layer overlays, the procedure described in "How to create three-color overlays of your fluorescent pictures using Adobe Photoshop" was followed using Adobe Photoshop CS2 version 7.02 (Morris, 2012). The image "MS KS 1 tubulin.tif," from the ICUC server was chosen for analysis because embryos depicted are in different phases of mitosis and images are clear. To analyze this image, the software ImageJ version 1.40g was used. The image was first opened using ImageJ. Then, using the line tool, a line was drawn across one of the embryos starting on black and ending on black to normalize the plot profile created from the line. This line was along the longest axis that crossed through the center of the embryo. If multiple axes were possible, then the axis that contained the most localized areas of bright green was chosen. Then, the plot profile of that line was created by selecting "Plot Profile" under the "Analyze" menu. This process was repeated for all of the embryos in the image.

Results

Figure 1 shows an overlay of green alpha-tubulin staining and blue DNA staining.
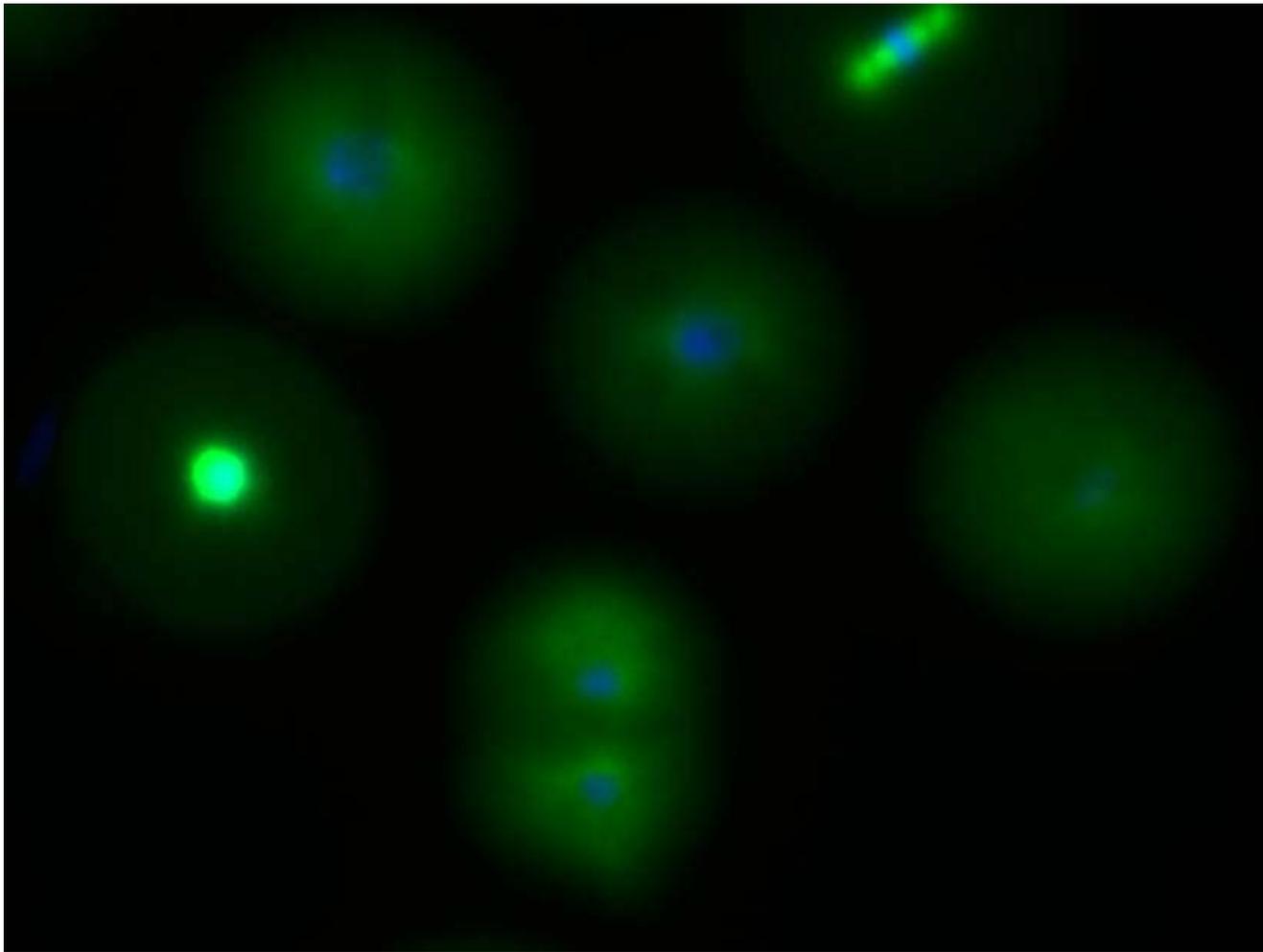
Figure 1: Overlay of blue fluorescing Hoechst labeled DNA image and green fluorescing FITC labeled alpha-tubulin image in sea urchin embryos. Embryos were fixed in methanol and are undergoing first mitosis. Images were taken at 40x magnification.

The staining in Figure 1 shows the locations of blue DNA and green alpha-tubulin in six embryos. Five embryos have only one DNA stain and are circular and similar in size. The sixth embryo is elongated and has two DNA stains. Alpha-tubulin, is localized in one or more regions in the embryos its arrangement varies.

The image used for the analysis of green-stained alpha-tubulin is Figure 2.
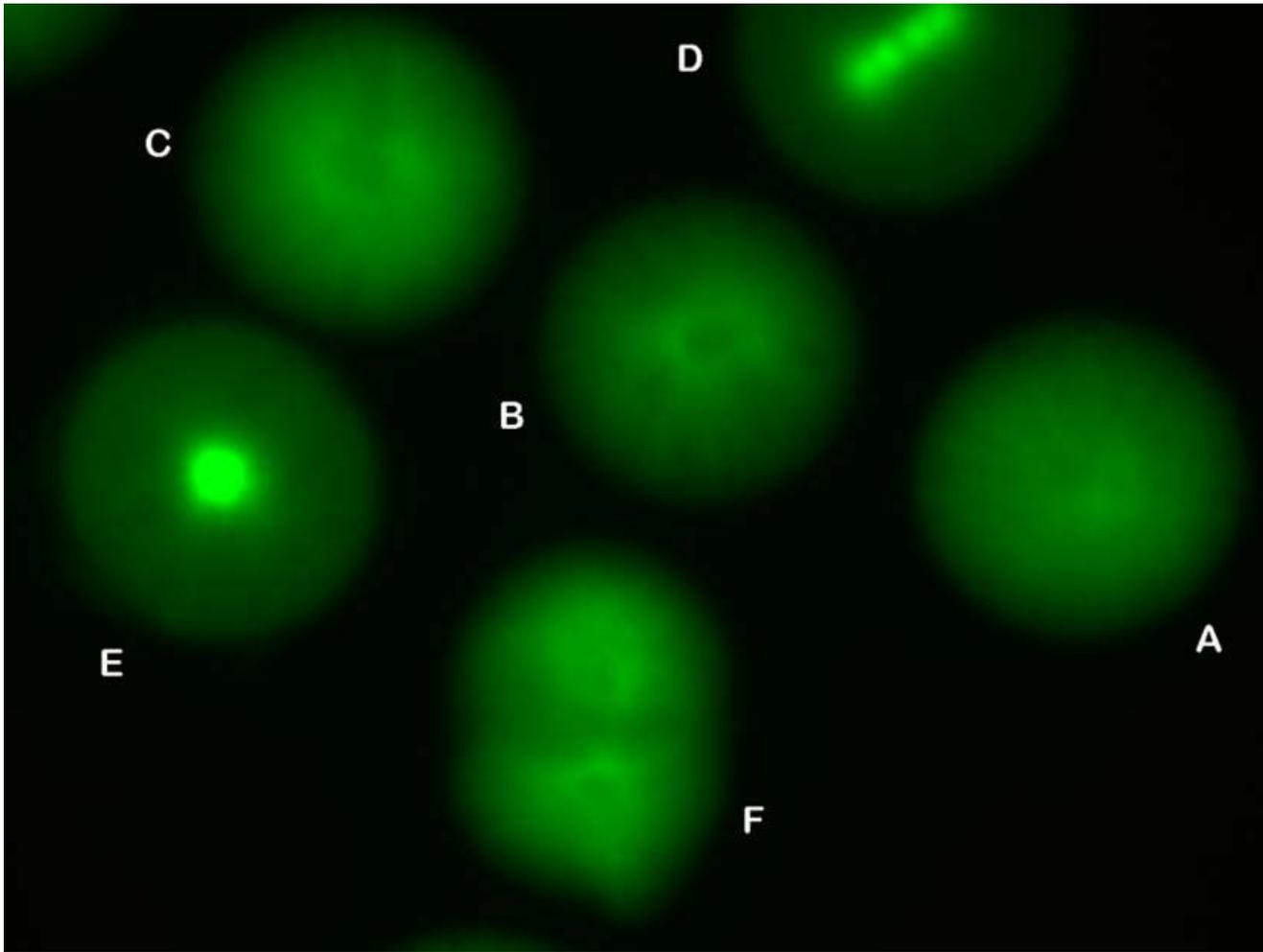
Figure 2: Green fluorescing FITC labeled alpha-tubulin image of sea urchin embryos at first mitosis stage. Embryos were fixed in methanol and the image was taken at 40x magnification. Image was quantified prior to the addition of alphabetic labels. Labels added to correspond the graphs to the embryos.

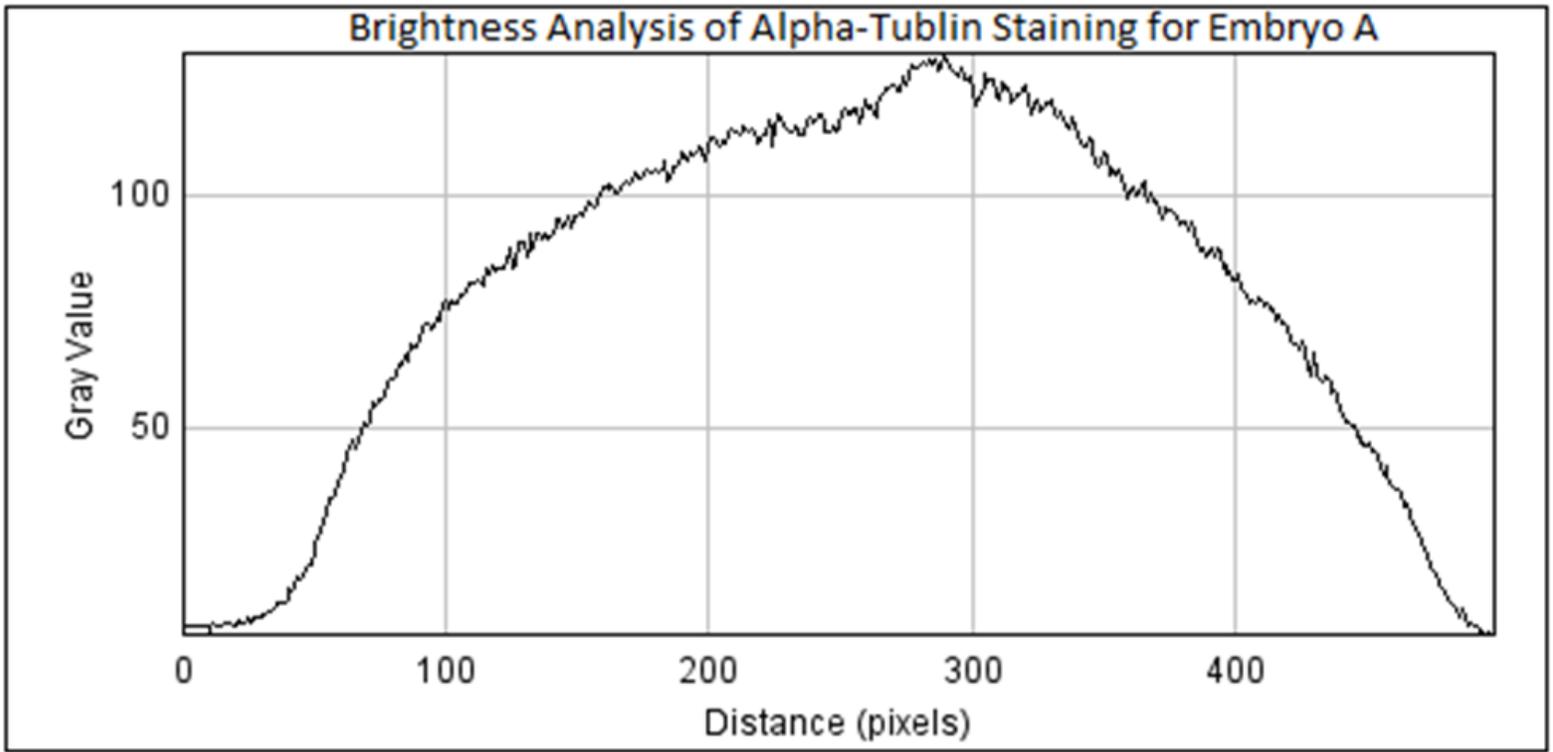The graphs of the brightness analyses are in Figures 3-8.

Figure 3: Plot profile of the embryo labeled "A" in Figure 2. Analysis was made by drawing a line across the embryo's longest axis and through the middle and performing a plot profile analysis for the line.
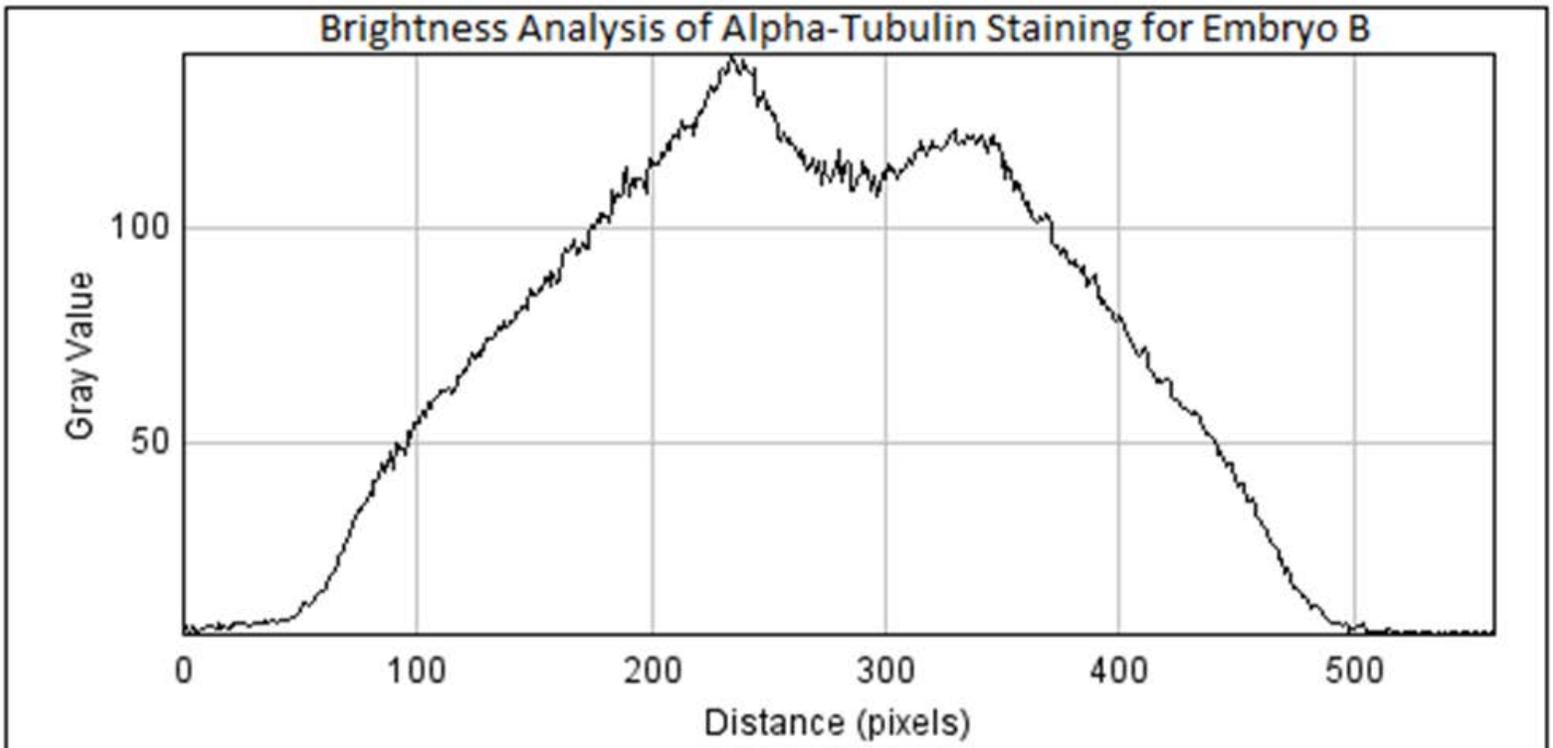

Figure 4: Plot profile of the embryo labeled "B" in Figure 2. Analysis was made by drawing a line across the embryo's longest axis and through the middle and performing a plot profile analysis for the line.
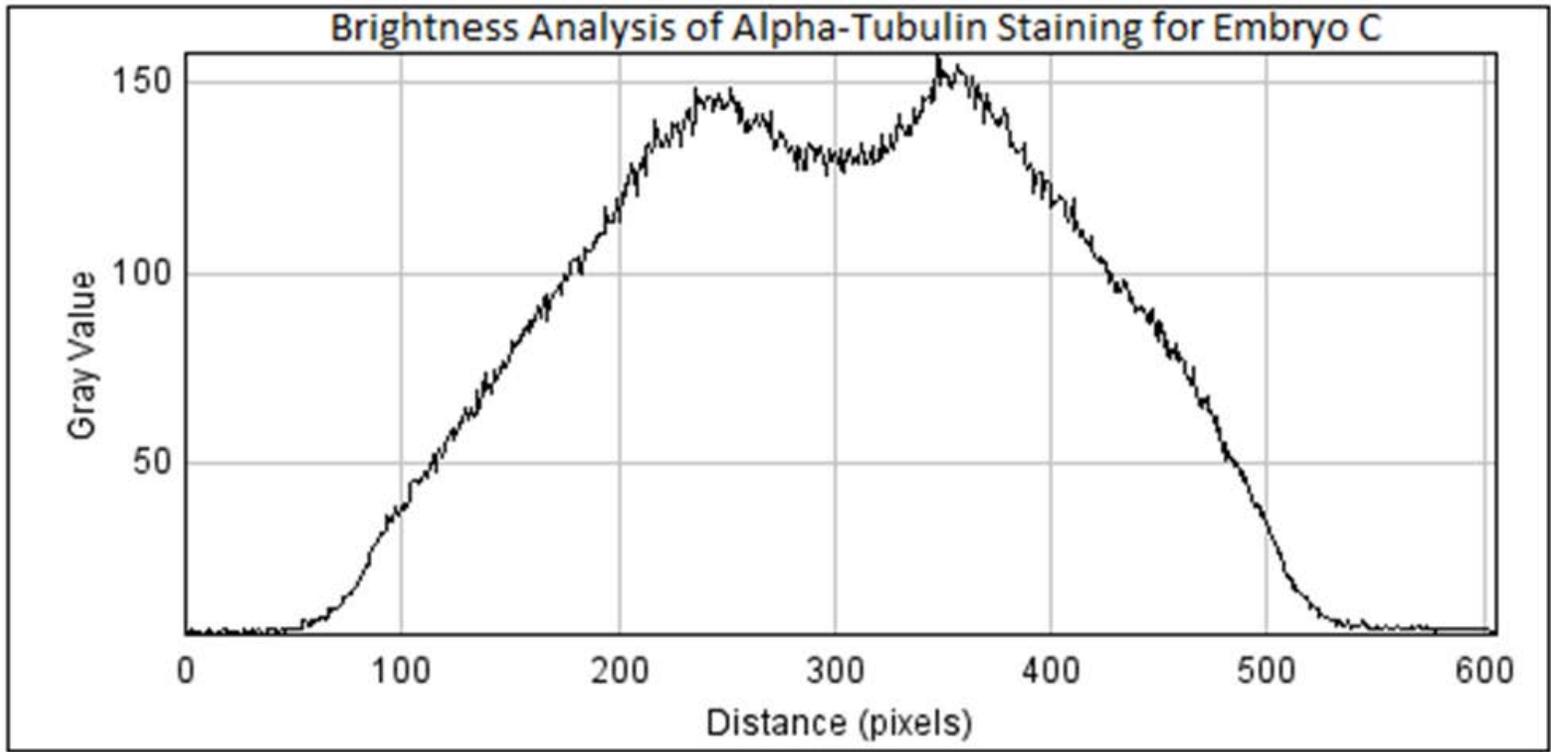
Figure 5: Plot profile of the embryo labeled "C" in Figure 2. Analysis was made by drawing a line across the embryo's longest axis and through the middle and performing a plot profile analysis for the line.
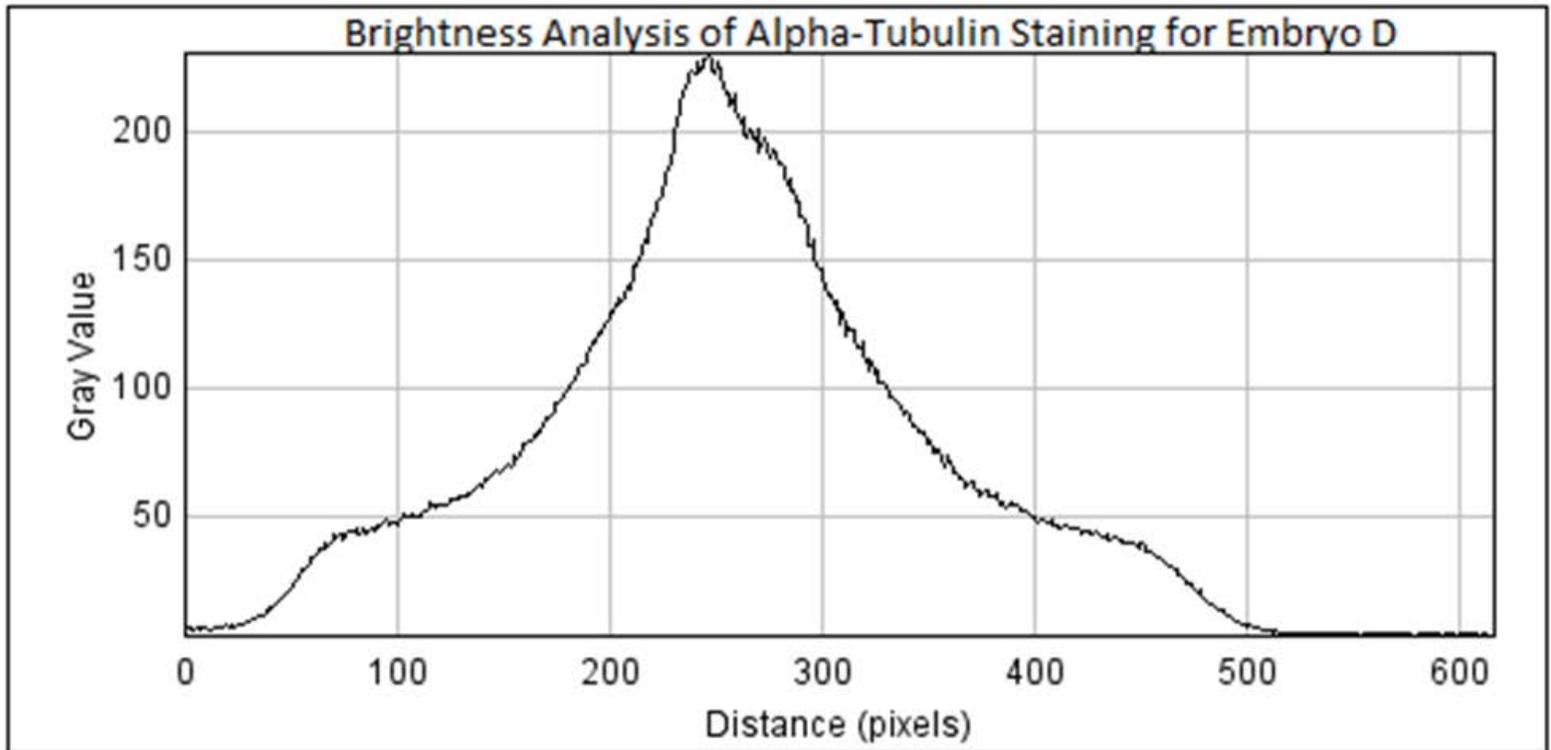

Figure 6: Plot profile of the embryo labeled "D" in Figure 2. Analysis was made by drawing a line across the embryo's longest axis and through the middle and performing a plot profile analysis for the line.

Figure 7: Plot profile of the embryo labeled "E" in Figure 2. Analysis was made by drawing a line across the embryo's longest axis and through the middle and performing a plot profile analysis for the line.
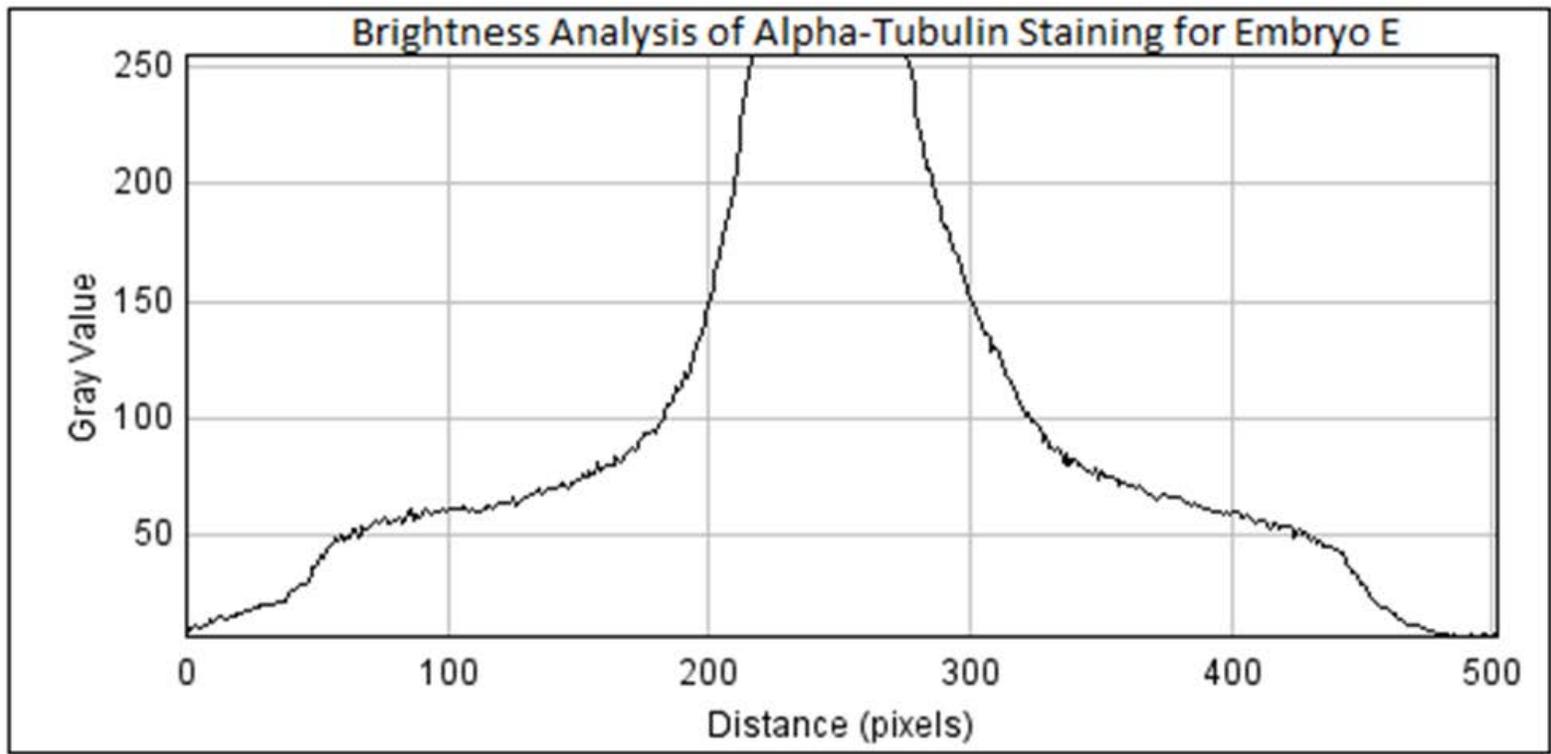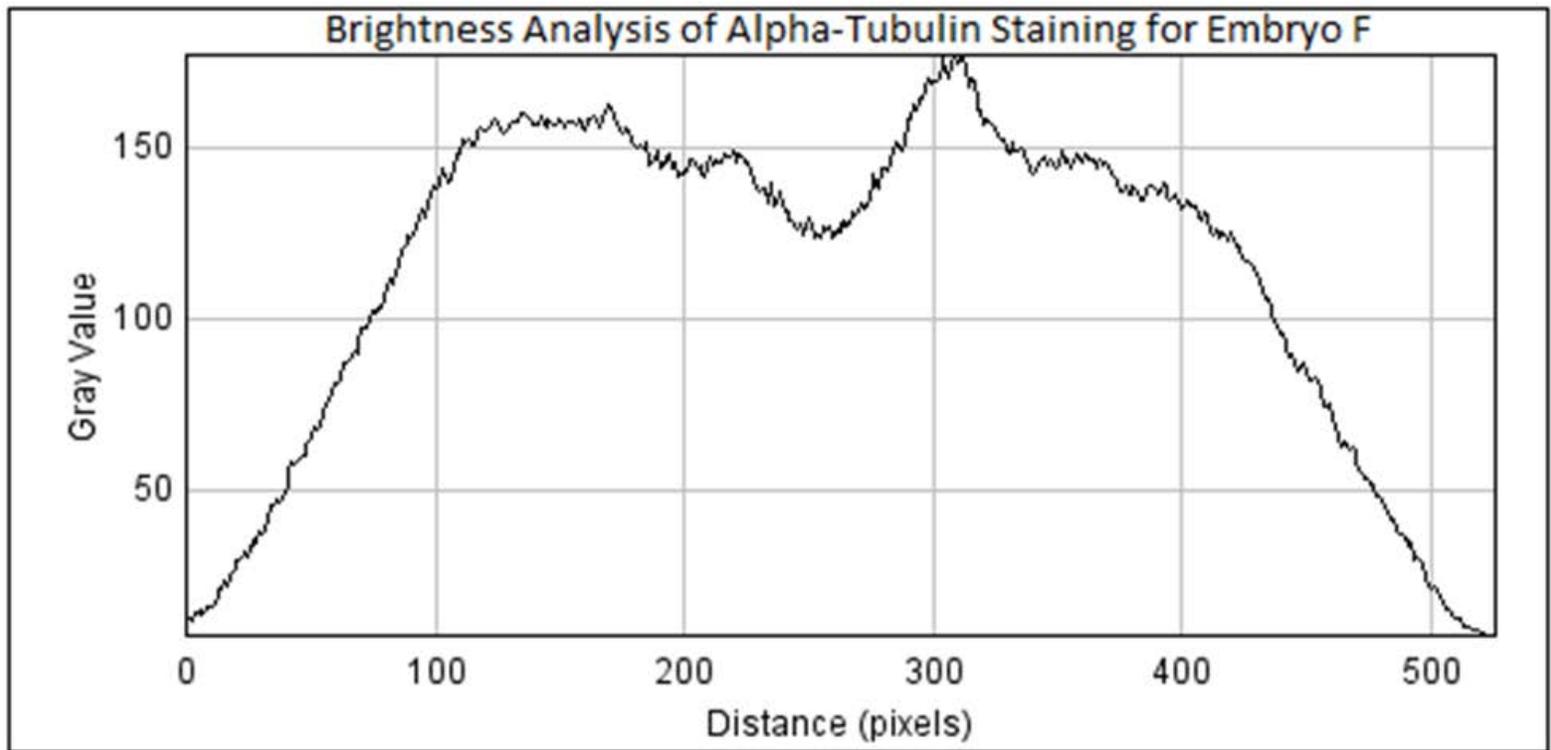

Figure 8: Plot profile of the embryo labeled "F" in Figure 2. Analysis was made by drawing a line across the embryo's longest axis and through the middle and performing a plot profile analysis for the line.

Gray Value measurements on the y-axis of Figures 3-8 represent the brightness at each pixel. The lowest value of 0 corresponds to black and the highest value of 255 represents white. The peaks on the graph correspond to the brightest areas of green across

the embryos in Figure 2. Figure 3 shows that embryo "A" gradually gets brighter towards the center to a rounded peak that then decreases moving away from the center. Figures 4 and 5 illustrate that embryos "B" and "C" gradually increase in brightness to a sharp peak, have lower in brightness at the center, and then peak again moving away from the center. Figures 6 and 7 show that embryos "D" and "E" are relatively dark on the edges of the embryos but have a sharp peak in brightness at the centers. Finally, Figure 8 shows that embryo "F" is bright across most of the embryo but does have a decrease in brightness at the center.

Discussion

Using the overlay image Figure 1 and the green α-tubulin fluorescence in Figure 2 it is possible to determine the phase of mitosis for the depicted embryos. Embryo "A" is in interphase because as seen in Figure 1, there is only one blue DNA stain and Figure 2 shows that there is α-tubulin extending radially from the one central location in the embryo. The centrally located α-tubulin represents the undivided centrosome (Amos, 2005). Subsequently, based on the microtubule arrangement in embryos "B" and "C" these embryos are in late interphase or possibly early prophase because in Figure 2, lines of α-tubulin originate from two brightly stained α-tubulin locations at the center of the cell. The brightly stained points at the center are the centrioles made of microtubules (Amos, 2005). The embryos depicted in Figure 2 as embryo "D" and embryo "E" are in the metaphase period of mitosis. From Figure 1, the embryo that corresponds to embryo "D" shows DNA located between two areas of very bright α-tubulin fluorescence indicative of high concentrations of α-tubulin. In metaphase, the chromosomes are lined up on the metaphase place between the two centrosomes, each of which contains two centrioles. In Figure 1, embryo "D" shows DNA localized between areas of high α-tubulin concentration. On each side of the DNA, there are two distinct and separate areas of α-tubulin that suggest the presence of two distinct centrioles. (Nigg, 2001). Embryo "E" is therefore also in metaphase, however the image is looking down the metaphase plate instead of at the metaphase plate. Finally, in embryo F, Figure 1 depicts two regions of DNA in the one cell that is still connected. This corresponds to the anaphase as the cell has not undergone cytokinesis and become two separate cells, yet there are two distinct regions of DNA (Nigg, 2001). Moreover, these assignments of phase based on microtubule arrangement correspond exactly to the phases described and depicted by Gundersen and Bulinski (1986).

These assignments for cell cycle stage combined with a comparison of the plots supports my hypothesis and suggest that α-tubulin arrangement is a useful predictor of mitotic phase. Embryos "B" and "C" are both in metaphase and have very similar plots of brightness as seen in Figures 4 and 5. In addition, embryos "D" and "E" are both in metaphase as predicted, their graphs of the brightness analysis demonstrate a similar shape with a very similar peak brightness value. The other embryos are all in different phases and as a result, the graphs of brightness across the embryo look different. Each phase of the cell cycle represented by an embryo has a graph that is distinctly different from the other graphs. Moreover, the graphs were

generated by computer software and represent quantized data. It is feasible that a standard plot profile of brightness across a cell could be generated for each stage in the cell cycle and that a computer could compare these standards with experimental measurements to determine what part of the cell cycle a specific cell is in, thus automating the analysis of the immunofluorescence. This conclusion appears to be supported by outside studies. For example, two separate studies found that automated analyses of immunofluorescence can be used to diagnose autoimmune diseases and the analyses were accurate when checked by humans performing the same analyses (Melegari, Bonaguri, Russo, Luista, Trenti, Lippi, 2012)(Kivity et al., 2011). In one of the studies, a system called AKLIDES analyzed results of anti-nuclear antibody, anti-double stranded DNA antibody, and anti-neutrophil cytoplasmic antibody immunofluorescence to diagnose autoimmune diseases. The AKLIDES system yielded the correct diagnosis of autoimmune diseases in 98.9% of the samples tested (Melegari, Bonaguri, Russo, Luista, Trenti, Lippi, 2012).

Applications of automating the determination of cell cycle might include the diagnosis of cancer. Cancer is a loss of regulation of the cell cycle and produces malignant tumors of cells that grow and divide rapidly (Alison, 2001). It would also be possible for a computer program to look a large sample of cells and provide sample statistics such as percentage of cells in each phase of mitosis. If a sample of tissue has a large number of cells actively undergoing mitosis when they should be in perpetual interphase it might be indicative of a cancer.

Future experiments that should be performed because of this conclusion might include making plot profiles for every phase of the cell cycle and performing the analysis on a large number of cells so that a definite pattern could be established. The next step would be to develop an algorithm for identifying the stage of cell cycle and then testing the automation process. Finally, experiments should be performed to discover if there is any diagnostic value for diseases such as cancer.

References

Amos, L. A. (2005). Tubulin and microtubules. In *Encyclopedia of Life Sciences*. Retrieved from http://0-onlinelibrary.wiley.com.helin.uri.edu/doi/10.1038/npg.els.0003890/full. doi: 10.1038/npg.els.0003890

Alison, M. R. (2001). Cancer. In *Encyclopedia of Life Sciences*. Retrieved from http://0-onlinelibrary.wiley.com.helin.uri.edu/doi/10.1038/npg.els.0001471/full. doi: 10.1038/npg.els.0001471

Gundersen, G.G., and Bulinski, J. B. (1986). Distribution of tyrosinated and nontyrosinated α-tubulin during mitosis. *The Journal of Cell Biology*, 102, 1118-1126.

Kivity, S., Gilburd, B., Agmon-Levin, N., Carrasco, M. G., Tzafrir, Y., Sofer, Y. … Shoenfeld, Y. (2011). *Clinical Rheumatology*, 31, 503-509. doi: 10.1007/s10067-011-1884-1

Melegari, A., Bonaguri, C., Russo, A., Luisita, B., Trenti, T., and Lippi, G. (2011). A comparative study on the reliability of an automated system for the evaluation of cell-based indirect immunofluorescence. *Autoimmunity Reviews*, n.v., n.p. doi: 10.1016/j.autrev.2011.12.010

Mertz, K. D., Demichelis, F., Kim, R., Schraml, P., Storz, M., Diener, P., Moch, H., and Rubin, M. A. (2007). Automated immunofluorescence analysis defines microvessal area as a prognostic parameter in clear cell renal cell cancer. *Human Pathology*, 38, 1454-1462. doi: 10.1016/j.humpath.2007.05.017

Morris, R. L. (2012, April). How to create three-color overlays of your fluorescent pictures using Adobe Photoshop. Retrieved from http://icuc.wheatonma.edu/bio254/2012/rmorris/How_to_create_three_color_overlays_in_photoshop.htm

Morris, R. L. (2012, April). Immunoflour staining of SU embryos – MeOH fixation. Retrieved from http://icuc.wheatonma.edu/bio254/2012/rmorris/Immunofluor_Protocol_2012.htm

Nigg, E. A. (2001). Mitosis. In *Encyclopedia of Life Sciences*. Retrieved from http://0-onlinelibrary.wiley.com.helin.uri.edu/doi/10.1038/npg.els.0001356/full. doi: 10.1038/npg.els.0001356